A Gel Electrophoresis Study of the Competitive Effects of Monovalent Counterion on the Extent of Divalent Counterions Binding to DNA

Anzhi Z. Li, Haiyan Huang, Xiaodan Re, Lai J. Qi, and Kenneth A. Marx
Department of Chemistry, University of Massachusetts, Lowell, Massachusetts 01854 USA

ABSTRACT The behavior of alkaline earth metal cations (Mg^{2+} and Ca^{2+}) and transition metal cations (Zn^{2+} and Cu^{2+}) interacting with λ-DNA-*Hin*dIII fragments ranging from 2,027 to 23,130 bp in Tris-borate-EDTA buffer solutions was investigated. The divalent counterions competed with $Tris^+$ and Na^+ for binding to polyion DNA, and the competition binding situations were investigated by measuring the reduction of the DNA mobility, by pulsed- or constant-field gel electrophoresis. The interaction of Mg^{2+} with DNA was intensively studied over a wide range of Mg^{2+} concentrations. In addition, we examined the competition binding as a function of ionic strength and DNA size. To compare valence effects, we studied $Co(NH_3)_6^{3+}$ interaction with DNA fragments under conditions similar to that of Mg^{2+}. At relatively low Mg^{2+} concentration, the normalized titration curves of DNA mobility were well fit by Manning's two-variable counterion condensation (CC) theory. The agreement between the predicted value (total charge neutralization fraction θ) from Manning's CC theory and the data based on our measured DNA electrophoretic mobility reduction was consistent under our experimental conditions. In contrast to alkaline earth metal cations (Mg^{2+} and Ca^{2+}), different binding behaviors were observed for the transition metal cations (Zn^{2+} and Cu^{2+}). These differences highlight the usefulness of our reduced DNA electrophoretic mobility measurement approach to describing cation interactions with polyelectrolyte DNA.

INTRODUCTION

Over the last two decades much attention has been paid (Eichhorn and Shin, 1968; Granot and Kearns, 1982; Rhee and Ware, 1983; Braunlin et al., 1989; Langlais et al., 1990; Duguid et al., 1995; Duguid and Bloomfield, 1996; Labarbe et al., 1996; Li et al., 1997) to the investigation of divalent metal cations binding to DNA, in the presence or absence of monovalent counterions, because of the importance of this problem from both a biological (Granot and Kearns, 1982; Manzini et al., 1990; Labarbe et al., 1996) and theoretical perspective (Manning, 1977, 1978, 1981). Our focus, in the general area of interaction of divalent metal cations with DNA in aqueous solution, is on understanding the nature of counterion binding to polyelectrolyte DNA. We choose Manning's counterion condensation (CC) theory (Manning, 1977, 1978) to interpret our experimental system, because of its physical insight as well as its simplicity and applicability. Furthermore, CC theory suggests the present approach to the study of competition binding for a two cation species system. The bridge between experimental data and Manning's CC prediction is provided by extracting the effective polyion charge from electrophoretic mobility reduction data for DNA, which is related to the total fraction of charge neutralization in CC theory.

Received for publication 15 October 1996 and in final form 4 November 1997.

Address reprint requests to Dr. Kenneth A. Marx, Department of Chemistry, University of Massachusetts, One University Ave, Lowell, MA 01854. Tel: 508-934-3658; Fax: 508-934-3013; E-mail: Marxk@woods.uml.edu.

Dr. Re's present address is Cambridge Technology Partners, 304 Vassar St., Cambridge, MA 02139.

© 1998 by the Biophysical Society

0006-3495/98/02/964/10 $2.00

Here we briefly review some concepts and equations of Manning's CC theory that are necessary for analyzing our experimental data. Manning's CC concept of delocalized counterion binding (Manning, 1978) differs from the traditional concepts of site binding and ion screening interactions. In the delocalized counterion binding mode, the condensed counterions are mobile but restricted within a relatively small volume surrounding the DNA. It is well known that DNA is a highly charged polyion, which tends to lower its charge density by counterion binding until the electrostatic repulsion energy no longer exceeds the limit of thermal energy (Manning, 1978).

The electrophoretic mobility reduction of the polyion is a measurable quantity that reflects the change of the net DNA charge due to counterion binding (i.e., the binding of counterions to DNA lowers its effective charge). The charge density parameter ξ is the important parameter governing counterion binding. It is given by $\xi = q^2/\epsilon k_b T b$, where q is the protonic charge, k_b is the Boltzmann parameter, T is the temperature in Kelvins, and b is the average axial charge spacing. The total fraction of charge neutralization θ is a ratio of counterion condensed over the initial polyion charge. If the solution contains only one counterion species with valence Z, then we have $\theta = 1 - 1/Z\xi$ (Manning, 1978). Because for double-stranded DNA in aqueous solutions $b = 1.7$ Å and $\xi = 4.2$ at 25°C, we have $\theta = 0.76$, 0.88, 0.92, and 0.94, corresponding to counterions with $Z =$ 1, 2, 3, and 4, respectively. The residual charge fraction remaining uncompensated by bound counterions is 0.24, 0.12, 0.08, and 0.06 for monovalent, divalent, trivalent, and tetravalent counterions, respectively.

As mentioned before, we are more interested in Manning's two-variable CC system, where two species of counterions of different valences are present in solution to com-

pete for binding to the polyion. The two-variable CC theory more closely approximates real systems and is therefore more applicable to practical problems. Suppose monovalent and higher valence cations, either divalent or trivalent, compete with each other. The fraction of charge neutralized by monovalent θ_1 and higher valence cations θ_Z, where $Z = 2$ or 3, could be calculated by the following equations (Manning, 1978; Wilson and Bloomfield, 1979):

$$1 + \ln(1000\theta_1/C_1V_{p1}) = -2\xi(1 - \theta_1 - Z\theta_Z)\ln(1 - e^{-\kappa b}) \quad (1)$$

$$\ln(\theta_Z/C_Z) = \ln(V_{pZ}/1000e) + Z\ln(1000\theta_1 e/C_1V_{p1}) \quad (2)$$

where $Z = 2$ and $Z = 3$ if the higher valence cation is divalent or trivalent, respectively. C_1 and C_Z refer to the molar concentrations of monovalent and higher valence counterions. κ is the Debye-Hückel screening parameter (Cantor and Schimmel, 1980), which is dependent on the ionic strength I. e is the base of natural logarithms. V_{p1} and V_{pZ} refer to the volume per mole phosphate within which the condensed counterions are considered to be territorially bound. The calculation for V_{pZ} is given by

$$V_{pZ} = 4\pi eN_0(1 + Z)(\xi - Z^{-1})b^3 \quad (3)$$

with $Z = 1$, 2, 3, corresponding to V_{p1}, V_{p2}, and V_{p3}, respectively; and N_0 is Avogadro's number, where V_{pZ} was defined under the assumption that the counterions are at infinite dilution (Manning, 1977). Now we have the total charge neutralization fraction of the polyion $\theta = \theta_1 + Z\theta_Z$. The residual charge fraction of polyion DNA after compensation by the bound counterions is $1 - \theta$ or $1 - (\theta_1 + Z\theta_Z)$.

The electrophoretic mobility μ of polyion DNA with residual charge Q driven by electric field E is defined as $\mu = v/E = Q/f$, where v is the velocity and f is the frictional coefficient. In reality, the mobility of the polyion is altered by the associated counterion atmosphere while this polyion is migrating. For a spherical polyion with radius a, the modified model is given by

$$\mu = (Q/f)X(\kappa a)/(1 + \kappa a) \quad (4)$$

The Henry function $X(\kappa a)$ ranges between 1.0 and 1.5, whereas κa varies from zero to infinity (Rice and Nagasawa, 1961), which reflects the interaction between the polyion and the counterion atmosphere. The frictional coefficient f, as well as the expansion of the polyelectrolyte chain (refer to the size a), depends only on the ionic strength of the buffer solution (Tanford, 1967). From the Henry model point of view, we expect that the DNA mobility μ will depend only on its residual charge Q if the ionic strength is kept constant. In our experimental system, the higher valent cation C_2 (or C_3) competes with univalent cations C_1 in the buffer for binding to DNA.

Note that if the C_2 is limited within a very low concentration range (0–200 μM) compared to the fixed monovalent cation concentration C_1 and ionic strength I (10–30 mM), the presence of the higher valence cation would not significantly alter the ionic strength, because $C_2 \ll C_1$. Therefore, we have a simple relationship that connects the mobility reduction and the total fraction of charge neutralization when DNA migrates in a buffer solution containing both monovalent and multivalent cations:

$$\mu/\mu_0 = (1 - \theta)/(1 - \theta_0) \quad (5)$$

where μ_0 and θ_0 refer to the controls measured in the solution where only monovalent $Tris^+$ and Na^+ are present in the buffer. Then the total fraction of charge neutralization θ can be obtained from mobility reduction data by means of Eq. 5.

In a previous study we utilized this approach to investigate the mobility reduction of DNA fragments, measured by pulsed-field gel electrophoresis, in the presence of increasing concentrations of the trivalent cations $Co(NH_3)_6^{3+}$ and $spermidine^{3+}$ (Li et al., 1996). The measured mobility reductions expressed as total fraction of charge neutralization were found to agree well with those calculated from Manning's CC theory. Previous papers have studied divalent and univalent counterion competition binding to DNA (Granot and Kearns, 1982; Rhee and Ware, 1983; Manzini et al., 1990; Ma and Bloomfield, 1995). Some of these studies compared experimental results with Manning's CC theory, but only qualitative agreement was reached (Rhee and Ware, 1983; Manzini et al., 1990). One study (Granot and Kearns, 1982) reported data on the interaction of DNA with divalent Mn^{2+} and compared their data with two theoretical approaches: Manning's CC theory and the Poisson-Boltzmann (PB) equation. The agreement is good between experimental data and theoretical predictions of average neutralized charge fraction in the absence of monovalent counterions; but the agreement is rather poor when experimental data are compared with predictions from either Manning's CC theory or the PB approaches in the presence of monovalent counterions (competition binding). Another study (Ma and Bloomfield, 1995) showed good agreement between measured data and the prediction of CC theory.

In this study we have performed extensive investigations on the alkaline earth metal cation Mg^{2+} interacting with λ-DNA-*Hin*dIII fragments ranging in size from 2,027 to 23,130 bp in Tris-borate-EDTA (TBE) buffer solutions. The divalent cation Mg^{2+} competed with $Tris^+$ and Na^+ for binding to DNA fragments at different buffer conditions and over a wide range of Mg^{2+} concentration from 10 μM to 20 mM. The effects of ionic strength, divalent cation concentration, and the DNA size on the competition binding were measured and compared with Manning's CC prediction. To examine valence effects, we compare the binding of divalent Mg^{2+} and trivalent $Co(NH_3)_6^{3+}$ to DNA fragments.

In addition, we compare the binding of alkaline earth metals Mg^{2+} and Ca^{2+} and the transition metal cations Zn^{2+} and Cu^{2+} to λ-DNA-*Hin*dIII fragments. The results show that different binding behaviors are observed for the two different types of metal cations.

MATERIALS AND METHODS

DNA and reagents

Linear fragments of λ-DNA-*Hin*dIII (2.027 kb, 2.322 kb, 4.361 kb, 6.557 kb, 9.416 kb, and 23.130 kb) were purchased from New England Biolabs. The stock solution (200 μg/ml) was made by dilution with Tris/EDTA buffer (10 mM Tris HCl, 0.1 mM EDTA, pH 7.4), purchased from Mann Biotech. At least 1 h was allowed for equilibrium of the DNA-cation mixture before loading onto the gel. In the loading solution the concentration of divalent metal cations or trivalent $Co(NH_3)_6^{3+}$ was the same as that in the TBE buffer.

Hexammine cobalt (III) was purchased from Sigma Chemical Co.; $MgCl_2$ and other metal cations were purchased from General Storage (Germany). Those reagents were used without further purification. Molecular biology grade agarose was the product of International Biotechnologies. Two types of TBE gel buffer solutions were used in our experiments. One type used in most measurements was made in the laboratory; this had a 100-fold lower EDTA concentration than the commercial TBE, to reduce EDTA-metal binding at low metal concentrations. The compounds Tris, borate, and EDTA were all purchased from Bio-Rad. The concentration of the stock solution was made of 445 mM Tris-borate and 0.1 mM EDTA (5×), then diluted to 0.25×, 0.5×, and 0.75×. We will use TBE_1 in the following text to indicate this homemade Tris-borate-EDTA gel buffer solution to distinguish it from the commercial type. Commercial Tris-borate-EDTA (5× TBE) electrophoresis buffer was purchased from Sigma Chemical Co. The stock buffer solution was then diluted to 0.5× TBE gel buffer, consisting of 44.5 mM Tris-borate and 1 mM EDTA, or to 1× TBE gel buffer, consisting of 89.0 mM Tris-borate and 2 mM EDTA. In any single experiment, divalent metal cations or hexammine cobalt (III) were added during buffer dilution to the designed final ligand concentration before use in gel electrophoresis.

Pulsed-field gel electrophoresis

The DNA in a gel is subjected to a series of unidirectional pulses (Holzwarth et al., 1989) of length 2 s (pulse on), separated by a rest period of 6 s (pulse off), and the magnitude of the applied electric field was 10 V/cm during the on pulse. A 0.8% mini-thin agarose gel (1 mm) was used in all of our pulsed-field gel electrophoresis experiments. The preparation of the gel, sample loading, staining, photography, and mobility measurement are described in our previous study (Li et al., 1996), along with the electrophoresis cell and the pulsed field instrumentation.

Because the gel was cast in TBE_1 or TBE buffer (without adding multivalent metal ions), a 1-h prerun (4 V/cm constant field) was carried out without DNA loading to equilibrate the ion concentration between gel matrix and buffer solution (with a final concentration of multivalent metal ions). We were faced with the choice of adding the divalent ions to the gel solution before or after gelation. The first approach is a traditional way to cook the divalent ions with the agarose and TBE_1 buffer. However, we chose the second approach and utilized an electrophoresis prerun to reach the equilibrium of divalent ions in the gel and buffer solution for the following reasons. We prefer to cast a number of gels at one time, to keep the gel concentration and gel structure exactly the same, which may be influenced by variations in environmental factors such as temperature and humidity, and by the solute environment as well. The addition of a varying concentration of divalent ions could influence gel formation and its structure, thereby producing errors dependent on the divalent ion concentration (C_2). It is critical to have "identical" gels to perform counterion binding for varying concentrations of divalent ions (C_2) to get consistent data. We carried out a series of preruns as a function of prerun time at a fixed divalent ion concentration. The reduced mobility was found to reach a constant value within 30 min of prerun time and remained constant (data not shown). Therefore we chose the standard prerun time of 60 min for divalent ion equilibration.

TBE_1 or TBE was the buffer used in all electrophoresis runs at different concentrations. In the case of $Co(NH_3)_6^{3+}$, a 0.5× TBE was used; in the case of Mg^{2+}, three different buffer concentrations were used: 0.25× TBE_1, 0.5× TBE_1, and 0.75× TBE_1. The concentration of $Co(NH_3)_6^{3+}$ was controlled within the range up to 150 μM, and Mg^{2+} was within the range up to 400 μM, to ensure the least DNA conformational change. A typical total run time was 4 or 5 h, to ensure accurate measurement of the electrophoretic mobility of the DNA fragments. All measurements were performed at 21.5°C (only one case was at 24°C, which was Mg^{2+} interacting with DNA in 0.75 TBE_1 buffer solution). The electrophoretic mobility μ was calculated by the formula $\mu = d/Et$, where d is the distance traveled by DNA in μm, E is the electric field strength in V/μm, and t is the migration time in seconds when the electric field was on.

Constant-field gel electrophoresis

The concentrations of divalent metal ions were in the range (0–15 mM) when constant-field gel electrophoresis was applied. A 0.8% mini-thin agarose gel (1 mm) was used where divalent Mg^{2+} was the ligand and 0.5× TBE was the buffer (Fig. 1 *B*). The electric field strength was set at 5.0 V/cm (3.0, 4.0, 5.0, and 6.5 V/cm were tried, but the final results were not significantly different), and the run time was ~2 h at 21.5°C.

A 0.7% conventional agarose gel was used in the set of measurements to compare the binding behavior of Mg^{2+}, Ca^{2+}, Zn^{2+}, and Cu^{2+}, where 1× TBE buffer (89.0 mM Tris-borate and 2 mM EDTA) was used (Figs. 6 and 7). The electric field was set at 1.5 V/cm, and the run time was fixed at 7 h. The buffer was circulated through a water bath to control the temperature precisely at 17.5°C.

Ion environment calculation

To apply Manning's two-variable CC theory, where Eqs. 1 and 2 must be solved simultaneously, we first need to analyze the ion environment to get the correct ionic strength and the monovalent cation concentration in which DNA fragments were electrophoresed. In TBE_1 or TBE buffer, $Tris^+$ and Na^+ (associated with EDTA) are the monovalent cations; they compete with divalent cations to bind to DNA. Note that TBE_1 or TBE buffer is a partially neutralized system; the concentrations of charged Tris, borate, and EDTA are dependent on several factors, such as the molar concentration of the buffer, the pH, and the temperature. The pK_a of each compound was first corrected by the temperature when it was different from 25°C, where $pK_a = 8.06$ (Tris), $pK_a = 9.24$ (borate), and the four pK_{ai} values were 2.0, 2.67, 6.16, and 10.27 (EDTA). Tris is a particularly temperature-sensitive pH buffer. Calculations to get equilibrium concentration for each species in the buffer were carried out by a program written in Mathematica, based on

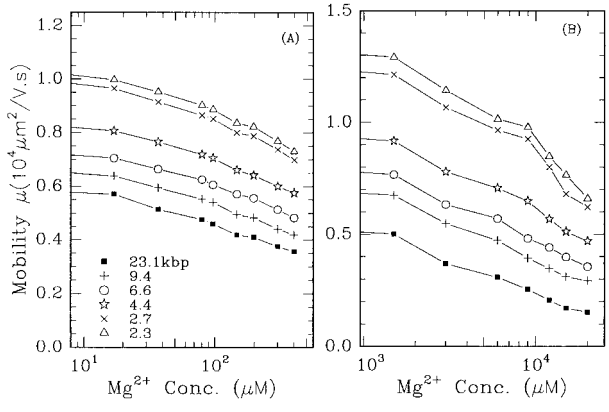

FIGURE 1 Electrophoretic mobility μ of λ-DNA-*Hin*dIII fragments (2.3–23.1 kbp) versus logarithm of the Mg^{2+} concentration. (*A*) Low Mg^{2+} concentration: a 0.8% agarose gel in 44.5 mM Tris-borate, 0.01 mM EDTA buffer, pH 8.2, 10 V/cm pulsed field. (*B*) High Mg^{2+} concentration: same type of gel as in *A*, but in 44.5 mM TBE buffer at 5.0 V/cm constant field.

the Henderson-Hasselbalch equation (Perrin and Dempsey, 1979), where the pK_a value was corrected iteratively to be pK_a' by the ionic strength effect and the Davies equation (Perrin and Dempsey, 1979).

For 0.5× TBE buffer containing 44.5 mM Tris-borate and 1 mM EDTA, at pH 8.2 ($Co(NH_3)_6^{3+}$-DNA interactions), the monovalent cation concentration C_1 was calculated to be 19.80 mM, and the ionic strength of the buffer system was 22.79 mM. In the cases of DNA-Mg^{2+} interactions, the ionic strength was changed systematically as follows: 1) 0.25× TBE_1 buffer (22.25 mM Tris-borate and 0.005 mM EDTA), the ionic strength was calculated to be 8.67 mM and C_1 was 8.65 mM; 2) 0.50× TBE_1 buffer (44.50 mM Tris-borate and 0.01 mM EDTA), the ionic strength was 17.70 mM, and C_1 was 17.67 mM; 3) 0.75× TBE_1 buffer (66.75 mM Tris-borate and 0.015 mM EDTA), the ionic strength for the buffer system was calculated to be 29.78 mM, and C_1 was 29.73 mM. Regarding the ion environment analysis, please refer to our previous publication (Li et al., 1996) for more details.

Competition binding calculation

The procedure is the same as in our previous publication (Li et al., 1996). First we calculate the Debye-Hückel screening parameter κ according to the known ionic strength, which is calculated by the Henderson-Hasselbalch and Davies equations. Then we compute the condensation volumes V_{p1}, V_{p2}, and V_{p3}, corresponding to the different valences $Z = 1, 2, 3$, respectively. We solve the simultaneous Eqs. 1 and 2 iteratively, using a program based on Mathematica (Wolfram, 1991) and substitute the known parameters, such as the condensation volume V_{pZ}, the monovalent cation concentration C_1, and the higher valence cation concentration C_2 (C_3) to get the charge neutralization fraction θ_1, θ_2 (θ_3), and the total fraction of charge neutralization θ. When the observed charge neutralization value was compared with the predicted value from CC theory, Eq. 5 was employed to convert the mobility reduction to the charge binding fraction, where $\theta_0 = 0.76$.

RESULTS

The investigations of counterion binding of divalent cations to DNA is based on the measurement of mobility reduction by gel electrophoresis due to each DNA fragment's charge being partially neutralized. Fig. 1 presents the picture that the mobilities of all λ-DNA-*Hin*dIII fragments were consistently lower as the metal cation Mg^{2+} concentration increased over a wide range. In Fig. 1 *A*, although the concentration (10–400 μM) of Mg^{2+} was relatively low compared to the ionic strength (17.70 mM), the mobility reduction reveals that this divalent cation competes strongly against the monovalent cations $Tris^+$ and Na^+ for binding to DNA. In Fig. 1 *B*, much higher concentrations (up to 20 mM) of Mg^{2+} were tested and present a similar picture. In Fig. 2 we present normalized electrophoretic mobilities μ/μ_0 comparing trivalent $Co(NH_3)_6^{3+}$ with divalent Mg^{2+} cation binding (in the presence of monovalent counterions), in the low multivalent cation concentration range of 10–200 μM. Below 200 μM we were able to directly compare the experimental data with Manning's CC prediction. The symbols indicate the measured mobility reduction from six fragments normalized by the control μ_0, which contained no cations other than $Tris^+$ and Na^+, and the solid line shows the calculated μ/μ_0 converted from θ, computed by Manning's two-variable CC theory. There is excellent agreement between the theoretical and experimental data for the

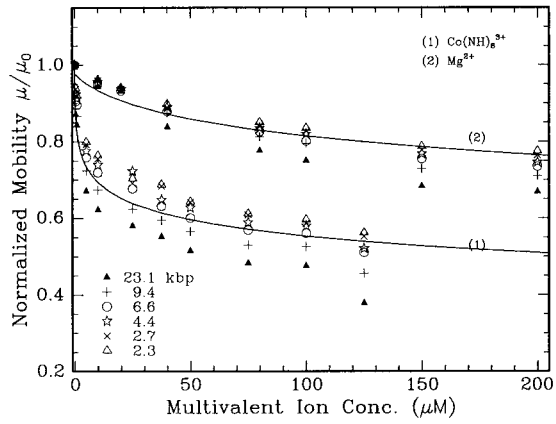

FIGURE 2 Normalized electrophoretic mobility μ/μ_0 of λ-DNA-*Hin*dIII fragments versus $Co(NH_3)_6^{3+}$ and Mg^{2+} concentration. *Curve 1*: A 0.8% agarose gel in 44.5 mM TBE buffer, pH 8.2, was electrophoresed at 10 V/cm pulsed field. *Curve 2*: The same gel conditions were used, but in 44.5 mM Tris-borate buffer with 0.01 mM EDTA. Fitting curves (*solid lines*) show the CC prediction, and symbols indicate the measured data.

two ions, even in the very low ligand concentration range. Only at the upper range of ligand concentration (125 μM for $Co(NH_3)_6^{3+}$ and 200 μM for Mg^{2+}) did the measured data begin to show more ion binding than the trend in the theoretical curves. These data show that both trivalent and divalent metal cations binding to DNA can be predicted and interpreted by Manning's CC theory, and the valence effect was also verified by the mobility reduction μ/μ_0 differences. Over the whole multivalent cation concentration range, at equivalent concentrations more $Co(NH_3)_6^{3+}$ than Mg^{2+} was bound to DNA fragments, lowering the DNA charge density and thereby lowering the mobilities.

The data presented in Fig. 3 show the total fraction of charge neutralization θ versus multivalent cation concentra-

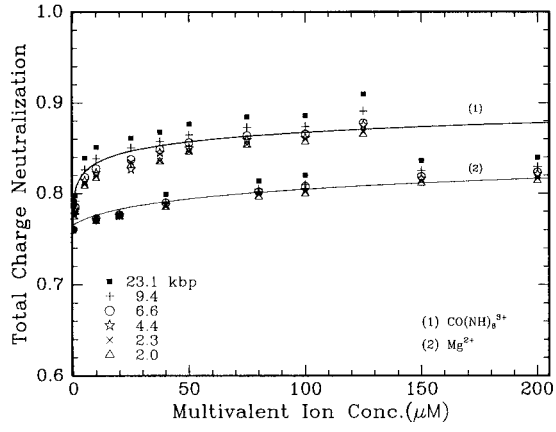

FIGURE 3 Comparison of the total charge neutralization fraction θ obtained from experimental measurements and two-variable counterion condensation theory. Binding of $Co(NH_3)_6^{3+}$ and Mg^{2+} to λ-DNA-*Hin*dIII fragments. *Curve 1*: $Co(NH_3)_6^{3+}$ at 22.79 mM ionic strength and 19.80 mM monovalent ion concentration. *Curve 2*: Mg^{2+} at 17.70 mM ionic strength and 17.67 mM monovalent ion concentration. The solid curves represent the two-variable CC prediction.

tion. The total fraction of charge neutralization θ calculated from CC theory depends on parameters of ionic strength, and higher valence and monovalent cation concentrations, and provides us information on binding competition. The binding competition condition is that the $Co(NH_3)_6^{3+}$ concentration ranges from 10 to 125 μM versus fixed 19.80 mM monovalent ion concentration in 22.79 mM ionic strength, whereas divalent Mg^{2+} concentration ranges from 10 to 200 μM versus 17.67 mM monovalent ion concentration in 17.70 mM ionic strength. The agreement between the CC prediction and experimental values is very good for both curves. For example, at 100 μM concentration, in the divalent case the observed values of θ were 0.800, 0.802, 0.803, 0.808, 0.809, and 0.820, corresponding to fragments 2.027 to 23.130 kb. The average θ is 0.807 for six fragments, whereas the calculated value is 0.805. In the trivalent case, the observed θ values were 0.857, 0.860, 0.861, 0.866, 0.874, and 0.886, corresponding to fragments 2.027 to 23.130 kb. The average θ is 0.867; the CC value is 0.867 also. Both experimental and predicted CC values show that trivalent ion has a higher binding fraction than does divalent ion. As shown in Table 1, ~0.06 greater charge fraction was neutralized in the $Co(NH_3)_6^{3+}$ case compared to Mg^{2+}. Although the ionic strengths were slightly different between the above two cases (divalent Mg^{2+} has lower ionic strength, which favors more binding), this difference will not influence the fundamental conclusion.

The ionic strength effect on the Mg^{2+} versus $Tris^+$ and Na^+ binding competition has been systematically investigated, and the results are presented in Fig. 4. As can be seen over the entire Mg^{2+} concentration range of 10–200 μM, the three curves show three different levels of mobility reduction due to Mg^{2+} binding to DNA fragments to different degrees governed by ionic strength, whereas other conditions are identical. Curve 3 shows the least mobility reduction. That would be the condition of the least Mg^{2+} binding, where the highest monovalent cation competition existed in the highest ionic strength condition (0.75× TBE_1). Curve 1 shows the greatest mobility reduction and highest Mg^{2+} binding under the buffer condition of 0.25× TBE_1, where the competitor monovalent cations $Tris^+$ and Na^+ had the lowest concentration. Curve 2 had the intermediate mobility reduction level, and its buffer concentration was 0.50× TBE_1. To show the experimental fragment mobility data (*symbols*) more clearly in a relatively crowded space, the symbols of curve 2 were set to be smaller than those in the other two curves, and the data points at concentrations 10, 20, 40, 100, 150, and 200 μM were shifted 3 μM lower. The three sets of curves were well fit by Manning's CC theory, where μ/μ_0 is converted from the calculated θ and reveals that the ionic strength effect is consistent between experimental values and Manning's CC theoretical predictions.

TABLE 1 Valence effect on the total fraction of charge neutralization θ (calculated)

	Ligand concentration C^{3+} and C^{2+} (μM)							
Valence	10	50	100	150	200	250	300	350
Tri. (+3)	0.834	0.857	0.867	0.873	0.878	0.881	0.884	0.886
Di. (+2)	0.776	0.794	0.805	0.811	0.816	0.821	0.824	0.827

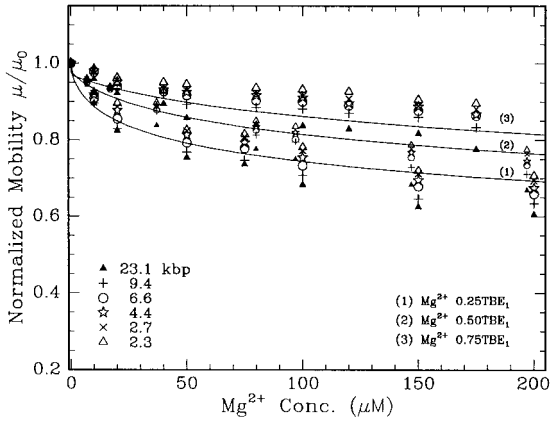

FIGURE 4 Ionic strength effect on divalent counterion binding. Normalized electrophoretic mobility μ/μ_0 for λ-DNA-*Hin*dIII fragments (*symbols*) versus Mg^{2+} concentration in different ionic strength conditions. DNA in a 0.8% agarose gel was electrophoresed in 22.25, 44.5, and 66.75 mM Tris-borate with 0.005, 0.01, and 0.015 mM EDTA buffer, respectively, at pH 8.2, 10 V/cm pulsed field. The experimental curves were fit by Manning's CC theory, shown by the solid lines.

Fig. 5, *A–D*, shows the charge neutralization fraction versus logarithm of ligand concentration over a wide range (0.01–400 μM). The theoretical curves were calculated from CC theory and show the competition between divalent/trivalent cations and monovalent cations directly. Note that the diamond symbol curve represents the total fraction of charge neutralization θ contributed by monovalent and divalent (or trivalent) ions.

Fig. 5 *A* shows the competition picture of trivalent cation (0.01–400 μM) competing with monovalent cation (C_1 = 19.80 mM) and ionic strength of 22.79 mM. The monovalent charge fraction drops down rapidly, whereas the trivalent charge fraction rises at the same rate, and the two curves cross at 0.387 μM, where trivalent and monovalent have equal charge neutralization fractions. After this point, the trivalent totally dominates the binding competition.

The respective competition conditions in Fig. 5, *B*, *C*, and *D*, are divalent cations (0.01–400 μM) versus monovalent concentrations of 8.65 mM, 17.67 mM, and 29.73 mM at ionic strengths of 8.67 mM, 17.70 mM, and 29.78 mM, respectively. Obviously, the binding behavior of Mg^{2+} is somewhat different from the trivalent case, with the rising rates of charge neutralization fraction θ_2 for divalent being much slower than that (θ_3) of trivalent ions, and the same is true of the decreasing rate of θ_1 for the monovalent ion. The cross-point, where the divalent neutralization fraction equals the monovalent neutralization fraction, keeps increasing while the ionic strength increases; it is 12.98 μM in Fig. 5 *B*, 53.70 μM in Fig. 5 *C*, ,and 150 μM in Fig. 5 *D*.

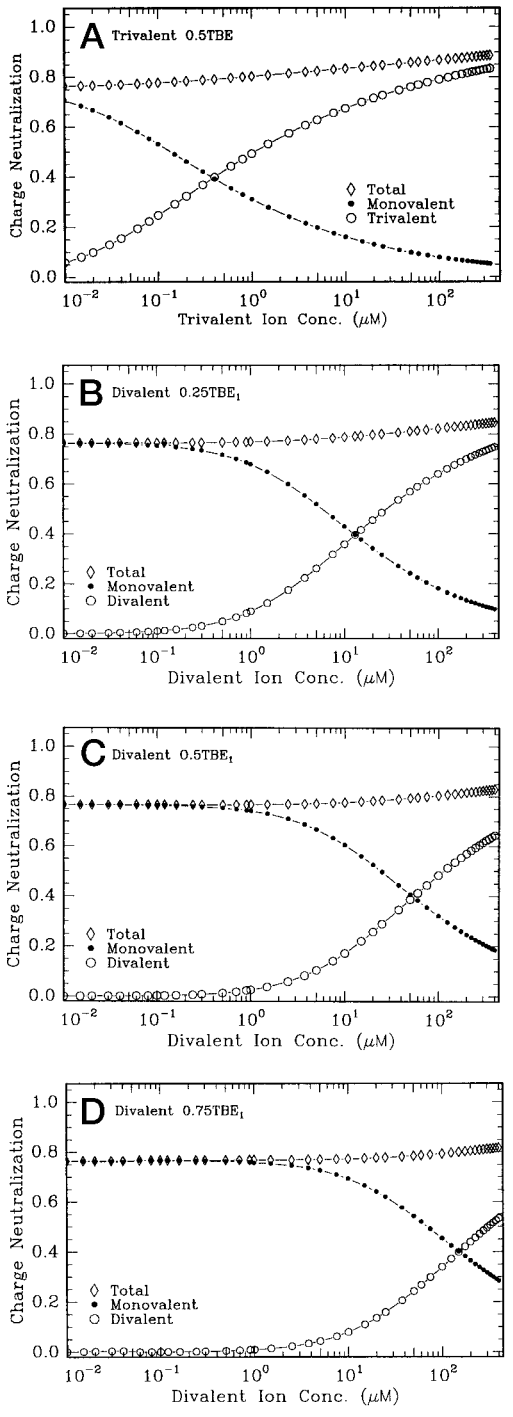

FIGURE 5 Ionic strength effect and valence effect on charge neutralization fraction θ, θ_1, and θ_2 (θ_3), calculated by CC theory. Charge neutralization fraction, θ, θ_1, and θ_2 (θ_3), versus logarithm of the $Co(NH_3)_6^{3+}$ or Mg^{2+} concentration under the following valence and ionic conditions: (*A*) $Co(NH_3)_6^{3+}$ in 22.79 mM ionic strength and 19.80 mM monovalent ion concentration; (*B*) Mg^{2+} in 8.67 mM ionic strength and 8.65 mM monovalent ion concentration; (*C*) Mg^{2+} in 17.70 mM ionic strength and 17.67 mM monovalent ion concentration; (*D*) Mg^{2+} in 29.78 mM ionic strength and 29.73 mM monovalent ion concentration. *B*, *C*, and *D* correspond to the 22.25, 44.50, and 66.75 mM Tris-borate and 0.005, 0.01, and 0.015 mM EDTA gel buffer conditions (Fig. 4), respectively. Curves represented by open circle, solid circle, and diamond symbols indicate the CC theory predicted charge neutralization fraction for θ_2 (or θ_3), θ_1, and θ, respectively.

A comparison of electrophoretically measured binding behaviors between the alkaline earth metal cations (Mg^{2+} and Ca^{2+}) and the transition metal cations (Zn^{2+} and Cu^{2+}) is presented in Figs. 6 and 7. The mobility of λ-DNA-*Hin*dIII fragments versus metal cation concentration (0–15 mM) for Mg^{2+}, Ca^{2+}, Zn^{2+}, and Cu^{2+} shows different patterns of mobility reduction and therefore different patterns of binding competition. For cations Mg^{2+} and Ca^{2+} (Fig. 6, *A* and *B*), the mobilities of all six DNA fragments decreased when the concentration of Mg^{2+} and Ca^{2+} increased. For the transition metal cation Zn^{2+} (Fig. 6 *C*), the mobility reduction was not as great as for Mg^{2+}. For the transition metal cation Cu^{2+} (Fig. 6 *D*), the pattern is very different from the others. The absolute mobilities of the λ-DNA-*Hin*dIII fragments decreased initially, then increased when the ligand concentration reached 5–6 mM. The same phenomenon was observed for this system with different electric field strengths (data not shown). In Fig. 7 we present normalized mobility μ/μ_0 versus cation concentration, which reflects the mobility reduction more directly. The three different patterns shown for mobility reduction reflect different patterns of binding competition. For example, at 12 mM metal cation concentration, the three smaller fragments (2.3, 2.7, and 4.4 kbp) had mobility reduction μ/μ_0 values of 0.62 for Mg^{2+}, ~0.67 for Ca^{2+}, but 0.87 for Zn^{2+} and 0.92 for Cu^{2+}. We would group the behavior of the alkaline earth metal cations Mg^{2+} and Ca^{2+} together. The transition metal cation Zn^{2+} is somewhat different, with Cu^{2+} being distinctly different in its concentration-dependent behavior.

DISCUSSION

Our previous paper (Li et al., 1996) has shown how meaningful the mobility reduction measurements by pulsed-field gel electrophoresis can be, providing a very simple and

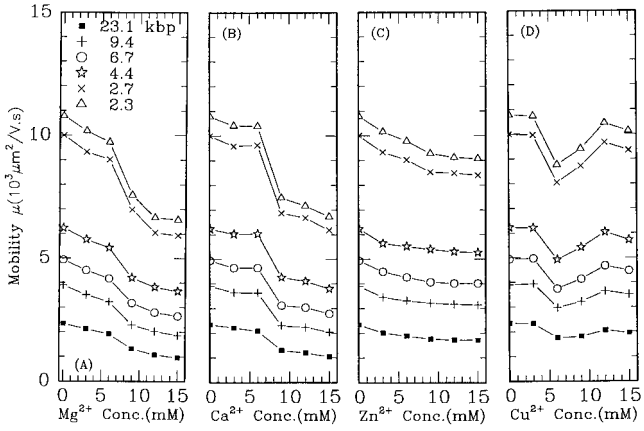

FIGURE 6 Comparison of the binding of metal ions Mg^{2+}, Ca^{2+}, Zn^{2+}, and Cu^{2+} to DNA. Electrophoretic mobility μ of the λ-DNA-*Hin*dIII fragments versus the metal ion concentrations. DNA in a 0.7% agarose gel was electrophoresed in 89.0 mM TBE buffer, at 1.5 V/cm constant field. (*A*) Mg^{2+}, (*B*) Ca^{2+}, (*C*) Zn^{2+}, (*D*) Cu^{2+}.

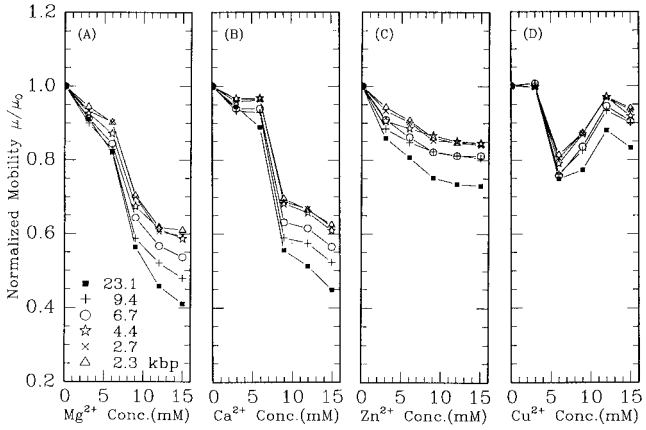

FIGURE 7 Normalized mobility μ/μ_0 of the λ-DNA-*Hin*dIII fragments versus the metal ion concentrations in the same conditions as Fig. 6. (*A*) Mg^{2+}, (*B*) Ca^{2+}, (*C*) Zn^{2+}, (*D*) Cu^{2+}.

practical way to determine the binding fraction of trivalent counterions to polyion DNA. In this paper, we expand the study to include divalent counterions of both alkaline earth metal and transition metal types. The results show that for alkaline earth metal cations such as Mg^{2+} and Ca^{2+}, the classical phosphate-binding behavior is roughly the same as for trivalent hexamine cobalt (III) and spermidine cations.

The following are important factors governing the competition binding: cation concentration, cation valence, ionic strength, DNA length, and divalent metal cation type.

Cation concentration effect

The binding fraction of divalent counterions could be measured from the DNA mobility reduction by pulsed-field gel electrophoresis. However, the mobility reductions were much smaller than observed for trivalent counterions and required more attention to the experimental design to get accurate data. We were unable to conduct the divalent counterion binding in the same buffer condition as $Co(NH_3)_6^{3+}$ (0.5× TBE containing 1 mM EDTA) because of significant complexation of divalent cations by EDTA. Measurements were tried with TB buffer, leaving out the EDTA. We were unable to obtain reproducible data in the absence of EDTA. With a 100-fold lower concentration of EDTA to reduce the EDTA-metal interaction, the experiments were carried out with consistent results. All experimental data (Figs. 2–4) were fit well by Manning's CC theory, and the agreement was excellent when Mg^{2+} concentrations were within the low concentration range (<200 μM) compared to the buffer ionic strength (~10–30 mM).

At very low concentrations of divalent cation, a sizable portion of divalent cations would be bound to EDTA, lowering the free divalent concentration. In this region (<20 μM) we would not expect very good agreement between measured and calculated mobility reduction. However, above this concentration region (>20 μM), free divalent concentration is near that of the added divalent concentration, and we find good agreement between the observed and predicted total fractions of charge neutralization.

The data (Fig. 1 *B* and Figs. 6 and 7) from large divalent cation concentrations (mM range) did not compare well with the CC prediction, because large C_2 will obviously change the magnitude of ionic strength, which we are assuming to be constant for CC calculations and comparison to experimental data. The condition of constant ionic strength must be met when applying Eq. 5 to equate the mobility reduction to the total fraction of charge neutralization from the gel electrophoresis data. Whereas the qualitative trend in mobility reduction continues for the experimental data at high divalent cation concentration, assumptions of constant ionic strength used in our model do not hold for these higher ligand concentrations. Therefore, we cannot apply CC theory calculations at these concentrations.

In the higher multivalent cation concentration experiments, 15 or 20 mM was the cation (Mg^{2+}, Ca^{2+}, Zn^{2+}, and Cu^{2+}) concentration limit. Beyond the upper limit, the bands of DNA fragments could not easily be detected. We would suggest that at large C_2 the DNA fragments would undergo a significant conformational change, and/or divalent cation binding could eliminate the ability of ethidium bromide to intercalate and visualize the DNA band through a strong competition effect.

Trivalent versus divalent

We compared the competition binding behavior of trivalent $Co(NH_3)_6^{3+}$ with divalent Mg^{2+}, both versus $Tris^+$ and Na^+ in electrophoresis buffer binding to λ-DNA-*Hin*dIII fragments. Fig. 2 shows that, except at very low ligand concentrations, the two curves possess similar shapes. We also noticed that the valence difference is much larger than the ionic strength differences with the same cation Mg^{2+}. In Fig. 2 the $Co(NH_3)_6^{3+}$ curve is lower than the Mg^{2+} curve at a nearly constant μ/μ_0 difference. Table 1 compares the total charge neutralization fraction between trivalent and divalent cations based on CC calculations. At 50 μM ligand concentration, the total fraction of charge neutralization θ is 0.794 for Mg^{2+} and 0.857 for $Co(NH_3)_6^{3+}$, and the difference is 0.063. At 100 μM ligand concentration, θ is 0.805 for Mg^{2+} and 0.867 for $Co(NH_3)_6^{3+}$, the difference being 0.062. At 200 μM ligand concentration, θ is 0.816 for Mg^{2+} and 0.878 for $Co(NH_3)_6^{3+}$, and the difference is still 0.062. With the basic concepts of Manning's CC theory (Manning, 1977, 1978) in mind, we know that the maximum total fraction of charge neutralized is limited eventually by the cation valence. For example, the θ_{max} value is 0.88 and 0.92 for the divalent and trivalent cations, respectively. The interpretation of these facts is that under normal temperature and aqueous solution conditions, even at very high ligand concentrations, divalent metal cations will not bring about the collapse of DNA, because a θ equal to or greater than 0.89 is required (Wilson and Bloomfield, 1979). Our data

clearly showed the valence difference between divalent and trivalent cations and that the data were fit well by Manning's CC theory, so the experimental data and CC theory show strong support for each other.

At certain cation concentrations, the charge neutralization fraction contributed by monovalent cations equals the fraction neutralized by the higher valence cations (trivalent or divalent). In Fig. 5 *A* this cross-point is calculated to be 0.387 μM for trivalent cations and 53.70 μM for divalent cations under very similar ionic environmental conditions. The cross-points are important references for viewing the competition picture, even though the above data were provided by calculation rather than measurements. Experimentally we can measure only the total fraction of charge neutralization, and so we cannot distinguish which portion is contributed by a particular valence cation. The concentration at which the cross-point occurs for divalent cations is greater than that of trivalent cations by about two orders of magnitude. From the values one can evaluate how rapidly the trivalent cation will dominate the competition relative to the much less effective divalent cation competitor.

Ionic strength effect

The CC theory was very effective at fitting data for the three ionic strength curves shown in Fig. 4, where divalent cation Mg^{2+} competed with $Tris^+$ and Na^+ at different ionic strengths. The good fit for small differences of ionic strength and fixed valence provides another example of the use of Manning's CC theory in application to DNA.

Table 2 presents the ionic strength effect on the total fraction of charge neutralization for divalent cation concentration (10–400 μM) competed with monovalent cation at a fixed concentration C_1 of 8.65 mM, 17.67 mM, and 29.73 mM in the ionic strength of 8.67 mM, 17.70 mM, and 29.78 mM, respectively. Experimental (Fig. 4) and CC predictions both show that the binding fraction decreases when the ionic strength increases, because the higher ionic strength corresponds to a smaller Debye-Hückel length ($1/\kappa$), resulting in a lower binding fraction. As mentioned before, the θ difference ($\Delta\theta$) due to ionic strength changes is much smaller than the effect due to a valence change (Table 1). The total charge neutralization difference $\Delta\theta$ is ~0.017–0.018 between ionic strength 8.67 mM and 17.70 mM and 0.012–0.013 between ionic strength 17.70 mM and 29.78 mM over a range of C_2 of 100–400 μM, whereas $\Delta\theta$ is ~0.062–0.063 between trivalent and divalent cations in a similar ionic environment. The curve shift (Fig. 4) reveals that higher divalent cation concentrations are required to reach a certain binding level when the ionic strength increases. For example, at an ionic strength of 8.67 mM (Fig. 5 *B*), 50 μM divalent cation results in a total charge neutralization fraction θ of 0.810 by prediction. If the ionic strength shifts from 8.67 mM to 17.70 mM (ΔI = 9.03 mM) (Fig. 5 *C*), it requires 150 μM C_2 instead of 50 μM, which is a threefold increase. And when the ionic strength shifts to 29.78 mM (ΔI = 12.08 mM) (Fig. 5 *D*), it requires 300 μM C_2 instead of 150 μM. Experimentally, the observed θ value based on measured mobility reduction μ/μ_0 showed a shift as well. In the lowest ionic strength (8.67 mM), a C_2 of 50 μM would result in a total charge neutralization fraction of 0.810 for the 6.7-kb fragment. After the ionic strength shifted to 17.70 mM, the Mg^{2+} concentration also shifted and a value between 100 and 150 μM was needed to reach the same binding level. For a further shift in the ionic strength to 29.78 mM, the Mg^{2+} concentration needed to reach the same binding level then was shifted to 350 μM. The agreement between the CC prediction and observed data regarding the divalent cation "shifting" phenomena due to changing ionic strength is very good.

We reached the conclusion that the binding fraction decreases when the ionic strength increases, as shown in Fig. 4 and Table 2. Could our interpretation of the ionic strength effect be confounded by the fact that the temperature in the gel increased with increasing ionic strength during gel electrophoresis? The temperature increases within the gel because of additional Joule heating, as a result of the increased electric current when ionic strength increases. Because the conductivity of the TBE_1 buffer will increase when ionic strength increases, this would produce additional Joule heating inside the gel.

First we analyze the specific experimental conditions in which the measurements were performed for an ionic strength effect, and realize that the temperature change due to additional Joule heating would be very small. We employed a mini-gel (1 mm thick), which is rather closer to the thermodynamic properties of a thin gel (Ansorge and Maeyer, 1980) than it is to the traditional agarose gel. According to these authors, there is a small temperature gradient across the gel thickness, efficient heat transfer, and rapid dissipation of Joule heating. On the other hand, pulsed-field gel electrophoresis was used for measurements (the ratio of field on to off time was 1:3), which favors the transfer of any Joule heating to the buffer reservoir and the surrounding air and eliminates the temperature difference between gel and buffer. Grossman and Soane (1990) esti-

TABLE 2 Ionic strength effect on the total fraction of charge neutralization θ (calculated)

Ionic strength (mM)	Divalent concentration C_2 (μM)								
	10	50	100	150	200	250	300	350	400
8.67	0.787	0.810	0.822	0.829	0.834	0.838	0.841	0.844	0.846
17.70	0.776	0.794	0.805	0.811	0.816	0.821	0.824	0.827	0.829
29.78	0.772	0.784	0.793	0.799	0.804	0.808	0.811	0.814	0.817

mated the temperature difference between the buffer in the center of a capillary and the surrounding air to be ~0.015°C, although their conditions are not identical to ours.

Counterion binding is not sensitive to small temperature changes. The calculations based on Eqs. 1 and 2 provide the following data. For example, when DNA interacting with divalent cations (100 μM) in 0.50× TBE_1 buffer has a 1°C temperature change (from 21.5°C to 22.5°C), the total charge neutralization fraction θ shifts from 0.8045 to 0.8046 and the $\Delta\theta/\theta$ is very small (0.00012). In 0.75× TBE_1 buffer, the $\Delta\theta/\theta$ due to a 1°C temperature change is found to be 0.00013.

An important point to mention is the fact that the two factors, ionic strength and temperature, effect counterion binding in opposite directions. Higher ionic strength, related to a smaller Debye-Hückel length ($1/\kappa$), results in a lower binding fraction θ, whereas increasing temperature corresponds to a larger Debye-Hückel length ($1/\kappa$), resulting in a higher binding fraction θ. Obviously, the temperature increase in a gel (if measurable) due to additional Joule heating from increasing ionic strength will increase θ very slightly, which does not favor the conclusion of our ionic strength effect. That the binding fraction decreases when ionic strength increases is only due to the ionic strength effect itself, not to its secondary effect.

DNA size effect

As we discussed before (Li et al., 1996), the experimental data show a distribution of total charge neutralization fraction θ or normalized mobility μ/μ_0, corresponding to DNA lengths from 2.0 to 23.1 kb, whereas the CC theory prediction provides only a single value (for an infinitely long polyion). All of the measurements showed consistent regularities: the larger the fragment length, the lower the mobility reduction, and the higher the total fraction of charge neutralization. We observed in Figs. 2, 3, 4, and 7 that the distribution of $\Delta(\mu/\mu_0)$ or $\Delta(\theta)$ over this molecular weight range was dependent on ionic strength, cation valence, and ligand concentration. More information and further discussion of this issue can be found elsewhere (Li et al., 1997).

Metal cation type

Figs. 6 and 7 compare the binding behaviors of four cations: Mg^{2+}, Ca^{2+}, Zn^{2+}, and Cu^{2+}. It was found that the binding behavior is similar for Mg^{2+} and Ca^{2+}, both alkaline earth metals. Different binding behaviors were observed for the transition metal cations Zn^{2+} and Cu^{2+}. The result is not surprising, because quite a few studies (Eichhorn and Shin, 1968; Daune, 1974; Langlais et al., 1990; Manzini et al., 1990; Re, 1991; Duguid et al., 1993, 1995) showed that alkaline earth metal cations and transition metal cations have different mechanisms of interacting with and binding to double-stranded DNA. From previous studies (Langlais et al., 1990; Manzini et al., 1990) it was concluded that alkaline earth cations interact primarily with DNA phosphates, resulting in stabilization of the double helix via reduction of electrostatic repulsion. In the former paper (Langlais et al., 1990), Raman spectroscopy shows that Mg^{2+} and Ca^{2+} interact dominantly with charged phosphates and very little with the bases. The other study shows that Ca^{2+} binding to DNA is independent of base sequence and can be interpreted by polyelectrolyte theory (Manzini et al., 1990). Our data of Ca^{2+} binding to the DNA fragments (Li et al., 1997) is well interpreted by Manning's CC theory, which includes only phosphate interactions, thus supporting the above obervation. Furthermore, our previous discussion of our Mg^{2+} data has shown that at low Mg^{2+} concentration, Manning's CC theory successfully accounted for the binding measurements.

In contrast, the transition metal cation Cu^{2+} is known to bind strongly to the DNA nitrogenous bases and destabilizes the double helix, promoting strand separation (Eichhorn and Shin, 1968; Rhee and Ware, 1983). It was classified with six other metal cations in the decreasing order Mg^{2+}, Co^{2+}, Ni^{2+}, Mn^{2+}, Zn^{2+}, Cd^{2+}, and Cu^{2+} for their binding affinity for phosphate groups rather than for the bases (Eichhorn and Shin, 1968; Langlais et al., 1990). In a study by Raman spectroscopy (Langlais et al., 1990), Zn^{2+} was found to be similar to Cu^{2+}, favoring base binding. Indirectly, through the mobility reduction in our measurements, the binding to the phosphate groups was examined (Fig. 6 and 7); the order is Mg^{2+} and $Ca^{2+} > Zn^{2+} > Cu^{2+}$, which is consistent with a reference (Langlais et al., 1990). In Figs. 6 and 7, the normalized electrophoretic mobility of DNA fragments first decreases when Cu^{2+} concentration increases; then it increases when the Cu^{2+} concentration continues increasing. This behavior may be accounted for in a two-step binding process. First Cu^{2+} interacts with phosphates, which brings about the normalized mobility reduction due to a reduced charge density. At increasing Cu^{2+} concentration, the metal primarily interacts with bases (Duguid and Bloomfield, 1996), causing local helix disruption and a total loss of double-helical conformational properties, resulting in the unusual μ/μ_0 reversal observed here. Our data show the difference of binding behavior between alkaline earth metals (Mg^{2+} and Ca^{2+}) and transition metals (Zn^{2+} and Cu^{2+}). However, the data presented here are not sufficient to construct a model to account for the binding mechanism of either transition metal cation, Cu^{2+} or Zn^{2+}, and further investigation is needed.

The authors acknowledge support from the Center for Intelligent Biomaterials. We also acknowledge the Biophysics Division, Nankai University, P. R. China, for their support, since a small portion of this work (Re and Li) was carried out there.

REFERENCES

Anderson, C. F., and T. M. Record, Jr. 1982. Polyelectrolyte theories and their applications to DNA. *Annu. Rev. Phys. Chem.* 33:191–222.

Ansorge, W., and L. D. E. Maeyer. 1980. Thermally stabilized very thin polyacrylamide gels for electrophoresis. *J. Chromatogr.* 202:45–53.

Braunlin, W. H., L. Nordenskiöld, and T. Drakenberg. 1989. The interaction of calcium (II) with DNA probed by ^{43}Ca-NMR is not influenced by terminal phosphate groups at ends and nicks. *Biopolymers.* 28: 1339–1342.

Cantor, C. R., and P. R. Schimmel. 1980. Biophysical Chemistry. Part II. Techniques for the Study of Biological Structure and Function. W. H. Freeman and Co., San Francisco.

Daune, M. 1974. Interactions of Metal Ions with Nucleic Acids. Metal Ions in Biological Systems. Marcel Dekker, New York.

Duguid, G. J., and V. A. Bloomfield. 1996. Electrostatic effects on the stability of condensed DNA in the presence of divalent cations. *Biophys. J.* 70:2838–2846.

Duguid, G. J., V. A. Bloomfield, J. Benevides, and G. J. Thomas, Jr. 1993. Raman spectroscopy of DNA-metal complexes. I. Interactions and conformational effects of the divalent cations: Mg, Ca, Sr, Ba, Mn, Co, Ni, Cu, Pd, and Cd. *Biophys. J.* 65:1916–1928.

Duguid, G. J., V. A. Bloomfield, J. M. Benevides, and G. J. Thomas, Jr. 1995. Raman spectroscopy of DNA-metal complexes. II. The thermal denaturation of DNA in the presence of Sr^{2+}, Ba^{2+}, Mg^{2+}, Ca^{2+}, Mn^{2+}, Co^{2+}, Ni^{2+}, and Cd^{2+}. *Biophys. J.* 69:2623–2641.

Eichhorn, G. L., and Y. A. Shin. 1968. Interactions of metal ions with polynucleotides and related compounds. XII. The relative effect of various metal ions on DNA helicity. *J. Am. Chem. Soc.* 90:7323–7328.

Granot, J., and D. R. Kearns. 1982. Interactions of DNA with divalent metal ions. III. Extent of metal binding: experiment and theory. *Biopolymers.* 21:219–232.

Grossman, P. D., and D. S. Soane. 1990. Orientation effects on the electrophoretic mobility of rod-shaped molecules in free solution. *Anal. Chem.* 62:1592–1596.

Holzwarth, G., K. J. Platt, C. B. Mckee, R. W. Whitcomb, and G. D. Crater. 1989. The acceleration of linear DNA during pulsed-field gel electrophoresis. *Biopolymers.* 28:1043–1058.

Labarbe, R., S. Flock, C. Maus, and C. Houssier. 1996. Polyelectrolyte counterion condensation theory explains differential scanning calorimetry studies of salt-induced condensation of chicken erythrocyte chromatin. *Biochemistry.* 35:3319–3327.

Langlais, M., H. A. Tajmir-Riahi, and R. Savoie. 1990. Raman spectroscopic study of the effects of Ca^{2+}, Mg^{2+}, Zn^{2+} and Cd^{2+} ions on calf thymus DNA: binding sites and conformational changes. *Biopolymers.* 30:743–752.

Li, A. Z., H. Huang, and K. A. Marx. 1997. DNA end-to-end distance change due to divalent counterion condensation studied by pulse gel electrophoresis. Statistical Mechanics in Physics and Biology. *MRS Symp. Proc. Ser.* 463:67–72.

Li, A. Z., L. J. Qi, H. H. Shih, and K. A. Marx. 1996. Trivalent counterion condensation on DNA measured by pulse gel electrophoresis. *Biopolymers.* 38:367–376.

Ma, C., and V. A. Bloomfield. 1995. Gel electrophoresis measurement of counterion condensation on DNA. *Biopolymers.* 35:211–216.

Manning, G. S. 1977. Limiting laws and counterion condensation in polyelectrolyte solutions. IV. The approach to the limit and the extraordinary stability of the charge fraction. *Biophys. Chem.* 7:95–102.

Manning, G. S. 1978. The molecular theory of polyelectrolyte solutions with applications to the electrostatic properties of polynucleotides. *Q. Rev. Biophys.* 11:179–246.

Manning, G. S.. 1981. Limiting laws and counterion condensation in polyelectrolyte solutions. 7. Electrophoretic mobility and conductance. *J. Phys. Chem.* 85:1508–1515.

Manzini, G., L. E. Xodo, F. Fogolari, and F. Quadrifoglio. 1990. Secondary structure effects on the interaction of different polynucleotides with Ca^{2+}. *Biopolymers.* 30:325–333.

Perrin, D. D., and B. Dempsey. 1979. Buffers for pH and Metal Ion Control. Chapman and Hall, London.

Re, X. 1991. Gel electrophoresis study of the ionic effect of Mg^{2+}, Ca^{2+}, Zn^{2+}, and Cu^{2+} metal ions on DNA. Master's thesis. Nankai University, Tianjin, China.

Rhee, K. W., and B. R. Ware. 1983. DNA-divalent metal cation interactions measured by electrophoretic light scattering. *J. Chem. Phys.* 78: 3349–3353.

Rice, S. A., and M. Nagasawa. 1961. Polyelectrolyte Solutions. Academic Press, New York.

Tanford, C. 1967. Physical Chemistry of Macromolecules. John Wiley and Sons, New York.

Wilson, R., and V. A. Bloomfield. 1979. Counterion-induced condensation of deoxyribonucleic acid. A light-scattering study. *Biochemistry.* 18: 2192–2196.

Wolfram, S. 1991. Mathematica. A System for Doing Mathematics by Computer. Addison-Wesley Publishing Company, Reading, MA.